ASPECTS REGARDING VELOCITY DISTRIBUTION IN THE SECONDARY ZONE OF A GAS TURBINE COMBUSTOR

Constantin ROTARU, **Ionică CÎRCIU**, **Cornel ARAMĂ**,
Cristian George CONSTANTINESCU
"Henri Coandă" Air Force Academy, Braşov, Romania
DOI: 10.19062/1842-9238.2015.13.3.5

Abstract: *This paper deals with the modelling and simulation of the combustion in a turbojet engine in order to find the velocity distribution in the secondary zone of the flame tube. The Arrhenius relationship, which describes the basic dependencies of the reaction rate on pressure, temperature and concentration, has been used. Also, combustion efficiency has been defined and related to both the exhaust temperature and species concentration. Premixed laminar flames and the dependence of propagation rate on temperature and the fuel-air ratio have been highlighted. The main focus of this paper consists in a new configuration of the aircraft engine combustion chamber with an optimal distribution of gas velocity in front of the turbine. This constructive solution could allow a lower engine rotational speed, a lower temperature in front of the first stage of the turbine and the possibility to increase the turbine pressure ratio. Also, a higher thermodynamic cycle efficiency and thrust in comparison to traditional constant-pressure combustion gas turbine engines could be obtained.*
Keywords: *combustion chamber, aircraft engine, premixed combustion.*

1. INTRODUCTION

The aircraft engine combustor requires an inlet velocity which is much lower than that leaving the high-pressure compressor, so that the flow velocity must be greatly reduced between these engine components. Although the purpose of a flow diffuser is to reduce axial velocity in order to gain static pressure, this must be accomplished in a short axial distance and with a minimal loss of total pressure. The gas turbine combustor is viewed not only as the source of thermal energy required by the propulsion cycle, but also as a necessary flow path which must provide adequate flow stream to maintain the static pressure drop between the compressor bleed outlet and turbine inlet. The radial various jets support a difference in both static and total pressure across the liner, as the jets flow into a second control volume having a single radial boundary inside the liner wall [1]. The viscous dissipation of kinetic energy in all of the jets leads to an approximately uniform level of total pressure within the liner.

The effect of the perforated colander liner is to maintain a fixed level of total pressure between the upstream and downstream plenums.

Because the Mach numbers have low values within the combustor, except within jet cores, the difference between the static and total pressure is slight, and so it is convenient to consider the static pressure to be approximately constant within the liner [2].

2. TURBULENT ROUND JETS IN THE FLAME TUBE

The round jet holes in both the secondary and dilution ones must be sized to provide the correct blockage to not only support the required total pressure loss, but also to divide the air flow into the appropriate mass flow rates into the primary, secondary and dilution zones.

The combustor is required to convert the chemical energy of the fuel into thermal energy with the smallest possible pressure loss and with the least emission of undesirable chemicals.

To achieve this in a small volume it is necessary for the flow to be highly turbulent [9, 10]. Because the behavior of the burning process depends on the turbulence, while at the same time the energy release brings about large alterations in the turbulence properties, it is not possible to carry out the detailed computations for the three-dimensional flow in the combustor (fig. 1).

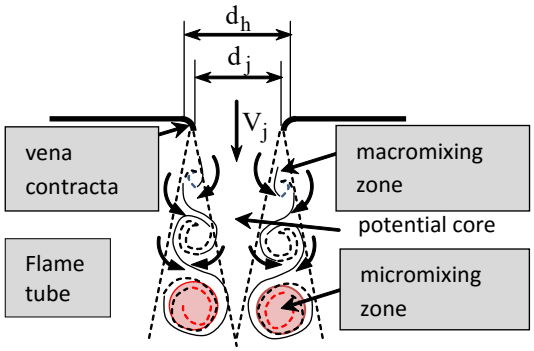

Fig. 1 Model flow in a combustor hole

If the flame tube region has a lower static pressure than the region above, the pressure difference causes a jet to flow through the hole of area $A_h = \pi d_h^2 / 4$, which reduced to $A_j = \pi d_j^2 / 4$. The vena contracta diameter d_j is approximately $(0.8 \div 0.9) d_h$. Because the flow is assumed to be isotropic, the jet velocity V_j is therefore determined by the static pressure difference. Downstream of the vena contracta all of the kinetic energy in the jet is converted to thermal energy by turbulence and subsequent viscous dissipation.

The length of the potential core varies from about $5d_j$ to $7d_j$ as the jet Reynolds number varies from 10^4 to 10^5 and the mixing transition point is about $10d_j$ downstream of the vena contracta [6, 7]. The micro mixed region occupies about one half the jet width, so that $\delta_m \cong 0.1\,y$ (fig. 2).

The combustor for a jet engine needs to be small to fit between the compressor and turbine without making the shaft unnecessarily long, since that would add to the weight and introduce problems of mechanical stiffness.

The high energy release in a small volume is made possible by the high pressure and by the very high level of turbulence created in the combustor which mixes the fuel and air [3, 4].

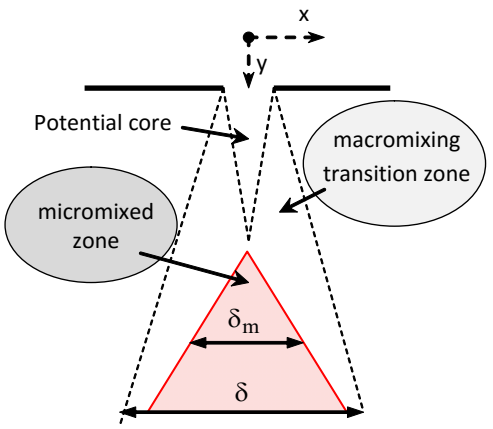

Fig. 2 Turbulent round jet

If all of the reactants are consumed in the combustion and there is no excess fuel or oxygen, the combustion is said to be stoichiometric.

A difficulty with hydrocarbon fuels is that they will not burn if the fuel-air ratio is far below stoichiometric. Fuel is injected as a fine sheet or spray and is broken up by a surrounding air blast. Most of the air from the compressor is diverted to avoid the region where the fuel is injected so that combustion starts in a relatively rich primary region with a fuel-air ratio of about 0.25 for takeoff and 0.1 at idle [8, 11]. Additional air is then fed in through holes in the combustor lining to complete the combustion process and to reduce the temperature to the level acceptable for the turbine so that after dilution, the effective overall air-fuel ratio is about 0.03. The air entering the dilution region also puts a layer of relatively cool air on the walls and modifies exit temperature radial profile to be suitable for entry into the turbine. To prevent the flame from being blown away it is necessary to set up local regions with much smaller velocity [5].

3. ENERGY RELEASE

Most frequently standard heats of formation are used to determine the chemical energy released during combustion process.

The standard heat of formation, h_f, represents the energy addition necessary for constant-pressure formation of a compound from its elements in their natural state at $25^\circ C$ and the energy required to accomplish any reaction can be calculated by algebraically summing the heat of formation contributions of the products minus the reactants

$$(\Delta h_r)_{25^\circ C} = \sum x_i (h_f)_i - \sum x_j (h_f)_j \quad (1)$$

where Δh_r represents the heat of reaction, x_i and x_j are the stoichiometric coefficients of product and reactant compounds.

The amount of heat, Δh_r, required to accomplish a reaction is a function of temperature. Heat required at temperature T_1, rather than $25^\circ C$ would be

$$(\Delta h_r)_{T_1} - (\Delta h_r)_{25^\circ C} = (h_{sp} - h_{sr})_{T_1} - (h_{sp} - h_{sr})_{25^\circ C} \quad (2)$$

where h_{sp} and h_{sr} are the product and reactant static enthalpies, respectively. For a given amount of energy release, it is apparent that the final flame temperature will increase with the initial temperature.

4. COMBUSTION PROCESS

Accurate flame temperature prediction requires consideration of the dissociation effects and variable specific heats. If the fluid in the annulus is moving from left to right at velocity U_A (fig. 3), then the fluid entering the jet carries with it its axial momentum flux in addition to the y direction momentum flux, $\rho_A V_j^2$, generated by the difference in static pressure. The entering velocity V_j is inclined at an angle θ, where $\theta = \arccos(U_A / V_j)$. An expression for the trajectory of the jet centerline is given by the equation [2]

$$\frac{y}{d_j} = 0.82 \left(\frac{\rho_A V_j^2}{\rho_L U_L^2} \right)^{0.5} \left(\frac{x}{d_j} \right)^{0.33} \quad (3)$$

The simplified relationship between the constant-pressure adiabatic flame temperature and mixture ratio is significantly altered when the detailed effects of dissociation and specific heat variations are included.

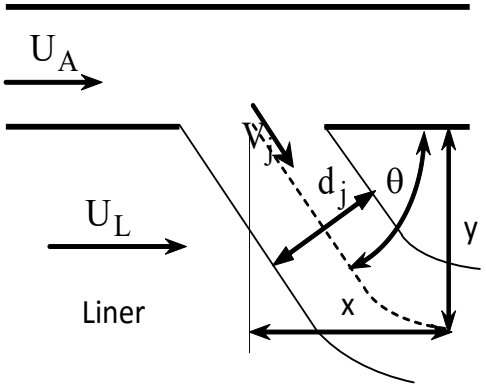

Fig. 3 Jet trajectory

The difference between the theoretical and actual flame temperatures as the mixture ratio approaches stoichiometric is due to the presence of significant O and H_2 concentrations at the higher temperatures.

The maximum combustion temperature occurs when hydrocarbon fuel molecules are mixed with just enough air so that all of the oxygen atoms are consumed, all of the hydrogen atoms form water vapor and all of the carbon atoms form carbon dioxide, this ideal mixture of fuel and air being represented by the atom-balance equation

$$C_x H_y + \left(x + \frac{y}{4} \right) \left[O_2 + \frac{79}{21} N_2 \right] \rightarrow x CO_2 + \frac{y}{2} H_2 O + \frac{79}{21} \left(x + \frac{y}{4} \right) N_2 \quad (4)$$

The stoichiometric mass-basis fuel-air ratio is given by

$$f_{st} = \frac{36x + 3y}{103(4x + y)} \quad (5)$$

A generic molecule representing jet fuels is $C_n H_{2n+2}$, which for $n = 12$ gives $f_{st} = 0.0669$ kg fuel/kg air. To quantify the off-stoichiometric mixtures of fuel and air, it is defined the fuel/air equivalence ratio, $\varphi = f / f_{st}$.

For the incomplete combustion, the atom-balance equation can be generalized as

$$C_xH_y+\left(x+\frac{y}{4}\right)\left[O_2+\frac{79}{21}N_2\right]\rightarrow\sum_{i=1}^{NS}n_iA_i \quad (6)$$

where NS represents the total number of product species, A_i represents the chemical formula of the i^{th} gas molecule appearing in the NS product gases and n_i represents the mass-specific mole number of the i^{th} species.

Methods for finding the actual composition of the post-combustion product gases, as represented by the set of mole number $\{n_i\}$, are provided by the software programs. Both the adiabatic flame temperature and heat of reaction are end-state quantities calculated on the basis of the static change from the given reactant mole numbers $\{n_i\}_R$ to the set of product mole number $\{n_i\}_P$. The product mole numbers can be calculated either from assumed complete combustion or chemical equilibrium.

Because fluid particle residence times in any subcomponent of a gas turbine engine are less than a millisecond, it is very often the case that insufficient time is available for the exothermic combustion reactions to reach chemical equilibrium.

If the two streams have different molecular identities, the shear layer is also a mixing layer and it is generated at the interface between the two streams, in which momentum is transported laterally from the faster to the slower stream (fig. 4).

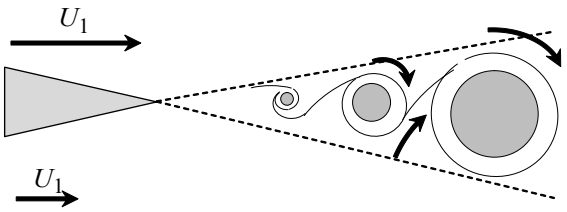

Fig. 4 Parallel streams mixing

The release of thermal energy occurs in three distinctly periods: the induction, heat release and equilibration regimes.

The induction period is the time interval immediately following some form of homogeneous bulk ignition, where the ignition occurs as a result of shock compression, but such ignition occurs only if the fuel and air are micro mixed to flammable proportions $(0.2<\phi<2.0)$.

The induction period ends when the mixture temperature begins to rapidly increase (after about 8×10^{-6} s). During the heat release period, the species equations and the energy conservation equations are strongly coupled. The heat release period ends when the reaction intermediates have all passed their peak values, at about 1×10^{-5} s. The equilibration period begins when all species mole numbers begin a decaying-exponential approach toward their respective equilibrium values. The end of the equilibration period can be defined as the time at which all of the mole numbers and the temperature are within 1% of their chemical equilibrium values, at about 5×10^{-4} s. Taking into account the combustion reaction progress variable, ε, the atom-balance equation for incomplete combustion, may be generalized as

$$\begin{aligned}&C_xH_y+\left(x+\frac{y}{4}\right)\left[O_2+\frac{79}{21}N_2\right]\rightarrow\\&\varphi(1-\varepsilon)C_xH_y+x\varphi\varepsilon CO_2+\frac{y}{2}\varphi\varepsilon H_2O+\\&+\left(x+\frac{y}{4}\right)\left[(1-\varphi\cdot\varepsilon)O_2+\frac{79}{21}N_2\right]\end{aligned} \quad (7)$$

For $\varepsilon=1$ in the above equation, the maximum value of T (the adiabatic flame temperature) is realized. The static temperature T and the reaction progress variable, ε, can be represented by the equation

$$T=T_i+\varepsilon\cdot\varphi\cdot\Delta T_{max} \quad (8)$$

where T_i is the air inlet temperature in the combustion chamber and ΔT_{max} is the maximum temperature rise when both $\varphi=1$ and $\varepsilon=1$.

The volumetric mass rate of consumption of the fuel, R_f, is expressed by the Arrhenius equation of the overall combustion reaction

$$\boldsymbol{R}_f = M_f\left(x+\frac{y}{4}\right)\varphi A e^{-\frac{T_{act}}{T}}\left(\frac{p}{RT\sum N_P}\right)(1-\varepsilon)(1-\varphi\cdot\varepsilon)$$

where M_f is the molecular weight of the fuel, A is the pre-exponential factor, T_{act} is the activation temperature of the reaction, p is the static pressure, R is the universal gas constant and $\sum N_p$ represents the sum of the product mole numbers given by the expression

$$\sum Np = \frac{100}{21}\left(x+\frac{y}{4}\right)+\varphi\left[1+\left(\frac{y}{4}-1\right)\varepsilon\right] \qquad (9)$$

On the other hand, the volumetric mass rate of consumption of the fuel can be expressed

$$\boldsymbol{R}_f = \left(\frac{\varphi\cdot f_{st}\cdot \dot{m}_A}{V}\right)\varepsilon \qquad (10)$$

where $\dot{m}_A$ is the mass feed rate of air and V is the volume of the combustor primary zone. The penetration depth of the secondary air jet trajectory is about ¼ the liner height, H_L (fig. 5).

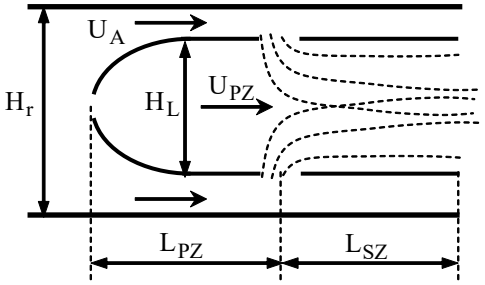

Fig. 5 Secondary zone trajectories

Because all of the secondary air must pass through round holes with jet vena contracta of diameter d_j, the number of the secondary holes is

$$N_{hSZ} = \frac{4\dot{m}_{SZ}}{\rho_r \pi d_j^2 V_j} \qquad (11)$$

The secondary air holes are spaced in a lateral line with one-half located on the upper flame tube wall and the other half, staggered and opposed, on the lower wall.

The axes of the secondary holes are located at the downstream end of the primary zone. The axial length of the secondary zone should be long enough for the inflowing jets to mix out the crossflowing primary zone effluent gases.

5. NUMERICAL RESULTS

The numerical simulations were made in Fluent software for a combustion chamber with a geometrical shape presented in the figure 6.

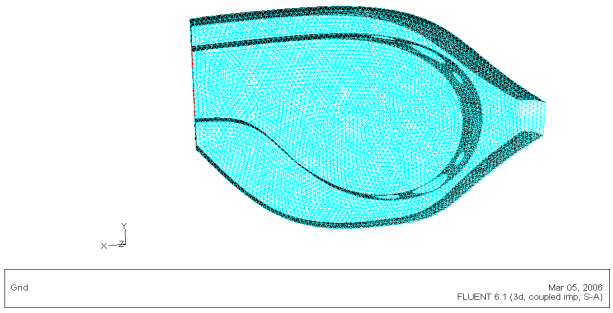

Fig. 6 Combustion chamber model

The velocity contours in the secondary zone of the flame tube and in the afterburner have the forms presented in the following pictures:

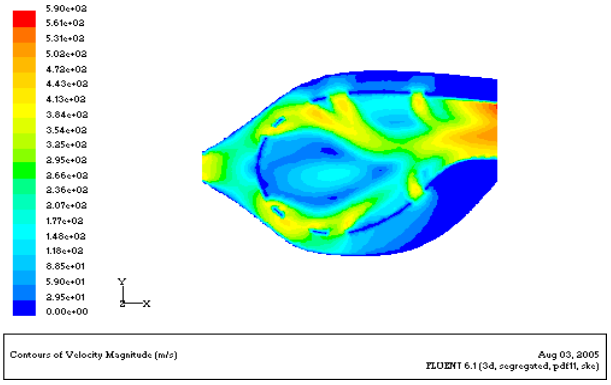

Fig. 7 Flame tube velocity contour

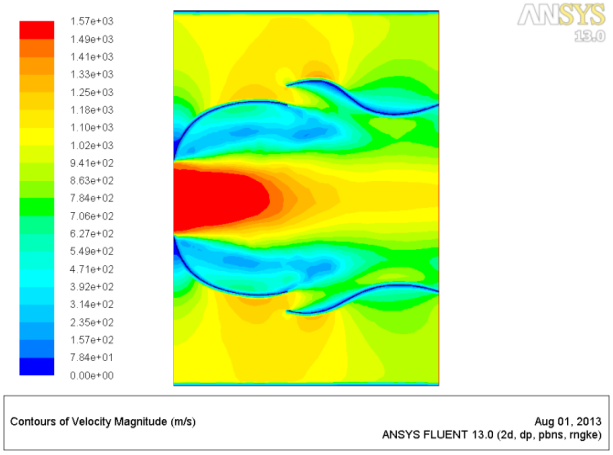

Fig. 8 Afterburner velocity contour

ACKNOWLEDGMENT

This paper has been financially supported within the project entitled "Gas Turbine using in situ combustion", contract number 286/01.07.2014 (PN-II-PT-PCCA-2013).

CONCLUSIONS

Any fluctuation in the heat input rate to a gas flow produces acoustic disturbances and variations in the entropy of the flowing gas. When these entropy variations are convected through a pressure gradient, a second acoustic disturbance is produced. The interaction of the traveling waves in this process will depend on the geometry and velocity distribution in the flame tube of the combustion chamber. A low turbulence intensity environment in a fuel-air mixture flow of 50-100 m/s results in a root mean square of the turbulence fluctuation speed of 2.5-5 m/s. In a high turbulence intensity in a flow with a mean speed of 100 m/s, the turbulence contribution to flame propagation speed may be as high as 30 m/s. The combustion model presented in this paper allows the study of the optimal shape of the combustion chamber.

BIBLIOGRAPHY

1. Farokhi, S., *Aircraft Propulsion*, John Wiley & Sons Inc., USA (2009).
2. Mattingly, J. D., *Elements of Propulsion. Gas Turbines and Rockets,* AIAA, Reston Virginia, USA (2006).
3. Moldoveanu, C. E., Giovannini A., Boisson H. C., *Turbulence receptivity of longitudinal vortex-dominated flows*, Lecture Notes in Computational Science and Engineering, Vol. 69: BAIL 2008 - Boundary and Interior Layer Proceedings of the International Conference on Boundary and Interior Layers - Computational and Asymptotic Methods, Limerick, Springer Verlag, Berlin, pag. 227 – 236, ISBN: 978-3-642-00604-3, (July, 2008).
4. Moldoveanu, C. E., Giovannini A., Boisson H. C., Şomoiag, P., *Simulation of Wake Vortex Aircraft in Ground Effect,* INCAS Buletin, Volum 3, nr. 1/2011, pag. 55-61, ISSN 2066-8201, (2011).
5. Moldoveanu, C. E., Moraru, F., Şomoiag, P., Boisson, H. C., Giovannini, A., *bulence Modelling Applied to Aircraft Wake Vortex Study*, MTA Review, Volum XXI, nr. 1/ 2011, ISSN 1843-3391, (2011).
6. Richter, H., *Advanced Control of Turbofan Engines,* Springer Science, USA, (2012).
7. Ronald, D. F., *Fundamentals of Jet Propulsion with Applications*, Cambridge University Press (2005).
8. Rotaru, C., "*Aspects Regarding Combustion Chamber Dynamics for Turbojet Engines*", ICMT'09 International Conference on Military Technologies, Brno, Czech Republic, Proceedings, pag. 342-349, (2010).
9. Rotaru, C., Arghiropol A., *Numerical Computation of Internal Flow for Turbojet Engine Combustion Chamber*, 16th International Conference The Knowledge-Based_Organization: Applied Technical Sciences and Advanced Military Technologies, Proceedings 3, pag. 117-122, Romania (2010).
10. Rotaru, C., Circiu, I., Boscoianu M. (2010). *Computational Methods for the Aerodynamic Design*, Review of the Air Force Academy, No 2(17), pp. 43-48, (2010).
11. Rotaru, C., Mihăilă-Andres, M., Matei, P. G., *An Extended Combustion Model for the Aircraft Turbojet Engine*, International Journal of Turbo & Jet Engines, Volume: 31, Issue: 3, Pages: 229-237 (Aug. 2014).